

# LOCALIZING AIRCRAFT NOISE SOURCES WITH LARGE SCALE ACOUSTIC ANTENNA

C.Cariou\*, O.Delverdier\*

\*AIRBUS Aircraft Physics Dpt, Toulouse

**Keywords:** *flight tests, exterior noise, sources localization*

## Abstract

The context of localisation tests is external noise campaigns for aircraft development purpose. Several extra flights are necessary with standard external noise tests to solve an acoustic exterior noise problem detected on ground. Localization tests produce a new type of results: they give access to the acoustic radiating energy distribution on the aircraft itself in the different flight configurations.

For this study, Airbus has worked with EADS-IW on quantification techniques and Company MicrodB to develop processing software. Airbus has set as an objective to develop a mobile and modular tool that could be installed in less than two days in any of the usual measurement sites for external noise.

## 1 Context of localization tests

### 1.1 Exterior noise campaigns

Several laboratories have worked for ten years on acoustic beamforming for aircraft flyover noise (eg. [1], [2]), and methods are still in evolution (eg. [3], [4]).

Exterior noise campaigns consist in measuring noise radiated from an aircraft during low altitude flyover above landing track with instrumentation installed on ground. Aircraft trajectory generally simulates approach or take-off procedures (see **Fig. 2**). A number of free-field microphones are placed at a 1,20m height from the ground in the trajectory axis and on both sides of the landing track. Since a few years, a large microphones array has been added

to standard instrumentation for development flights.



Fig. 1. Localisation measurement

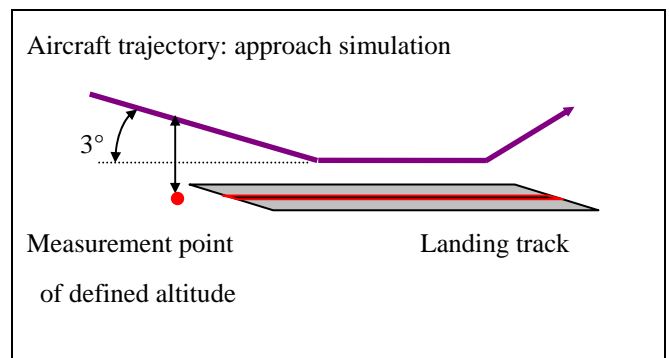


Fig. 2. Approach simulation

## 1.2 Advantages of localisation tool

Localization tool is a good complement to more conventional instrumentation, because it produces a new type of results: instead of evaluating the noise level received on ground, it quantifies the sources level in the aircraft plan. However, practical aspects have to be carefully optimized to renders this tool compatible with standard external campaigns: short installation time, good equipment safety, reliable radio-communication, etc...

One major objective of the tool developed was the performances at low frequency. Low frequencies are always a challenge in antenna measurements, because big size array is required to describe correctly large wavelength.

## 2 Three-steps calculations

The objective of the processing method is to build acoustic maps, taking as inputs:

- ✓ the acoustic signals recorded at the microphones of the antenna
- ✓ the trajectory data containing position of aircraft reference point and aircraft angles versus time
- ✓ the definition of the antenna and the exact positions of all microphones

The method then runs in three steps:

### 2.1 Radiation

Suppose an acoustic source  $s$  moving on a trajectory at a distance  $r_m^s(t)$  from a microphone  $m$ . The assumption is made of spherical radiation. At time of reception  $t+r_m^s/c$ , the signal registered at the microphone is:

$$p_m(t+r_m^s/c) = \frac{q_m(t, \vec{x}_s)}{4\pi M_m^s \times r_m^s} \quad (1)$$

Where  $q_m$  is the source flow. The amplitude of the signal is corrected by a Mach factor  $M_m^s$  depending on source velocity:

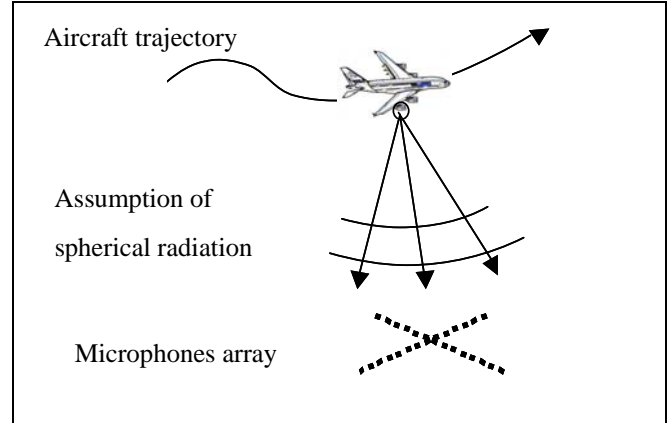


Fig. 3. Radiated noise measurement with microphones array

### 2.2 Beamforming

Radiated time signals are combined in order to focalise successively on each point of a virtual plan including the aircraft, and build a beamforming map. The beamformer is a summation of the measured pressures with delays corresponding to the distances to sources:

$$a(t, \vec{x}_f) = \sum_{m=1}^N w_m \frac{M_m^f \times r_m^f}{M_0^f \times r_0^f} p_m(t + r_m^f/c) \quad (2)$$

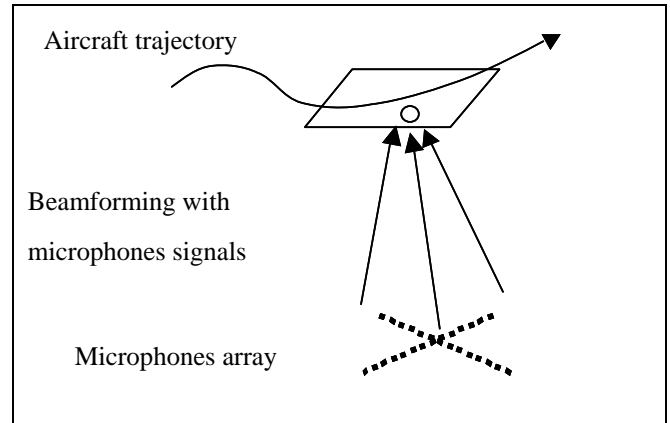


Fig. 4. Focalisation in aircraft plan

### 2.3 Quantification

The focalization step enables to identify sources locations on the aircraft, but does not give the true sources amplitudes because of the presence of the secondary lobes of each source.

A synthetic sources distribution is then optimized in the virtual plan in order to best fit to the beamforming results. Measured pressures of equation (2) are now replaced by an integration of the modelled sources distribution over the sources region S:

$$\iint_S \frac{q(t - r_m^s/c + r_m^f/c)}{4\pi M_m^s \times r_m^s} dS \quad (3)$$

After Fourier transform, the expression of quantification is written in a synthetic way in order to put into evidence the transfer functions between modelled sources and focus points  $G(\omega, x_f, x_s)$ :

$$A(\omega, \bar{x}_f) = \iint_S G(\omega, \bar{x}_f, \bar{x}_s) \times Q(\omega, \bar{x}_s) dS \quad (4)$$

Amplitudes of modelled sources  $Q(\omega, x_s)$  are obtained by identification with the beamforming expression (3). Sources are assumed to be uncorrelated between each other. The right amplitudes of modelled sources are obtained when the focalisation map computed with the modelled signals fits with the focalisation map obtained with the measured signals.

This quantification step requires more calculation time, but it gives the true amplitudes of the sources and improves greatly the spatial resolution. The linear system obtained for quantification is solved with a specific iterative gradient algorithm developed by EADS-CRC.

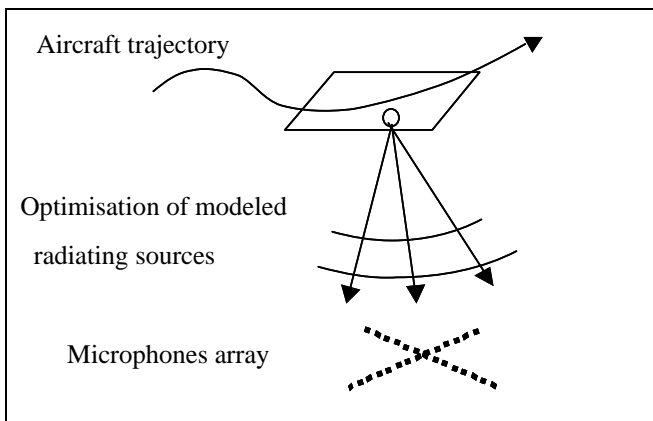


Fig. 5. Quantification of sources amplitudes

### 3 Results processing

#### 3.1 Elaboration of acoustic maps

In the following graphics, we show results obtained on a test aircraft at 90° incidence for third octave band 315 Hz. Definition of angles is given on **Fig. 6**.

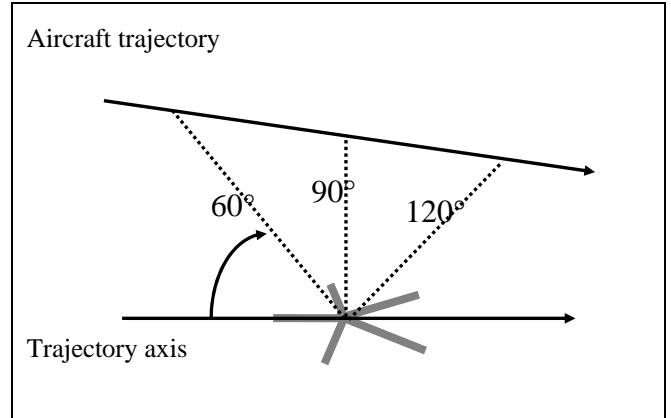


Fig. 6. Incidence angles for maps calculation

The beamforming map obtained from measurements is given on **Fig. 7** with 9dB dynamics. Quantification map is more accurate (**Fig. 8**) and is given with 16dB dynamics. Resolution is good despite the low frequency studied.

Last map (**Fig. 9**) is obtained by focalization with results of quantification. It is very similar to **Fig. 7** (and with same maximum level), which shows that quantification was successful.

#### 3.2 Sources comparison

Once the quantification maps has been calculated, it is possible to represent power spectra corresponding to power integration over predefined zones. An example of such ones is given on **Fig. 10**. On that same figure, a representation of focus plan meshing is given.

On **Fig. 11**, the power spectra of two engines at low frequency are compared to global noise of the right wing zone. The graphic is given with 5dB scale, and expressed with normalized frequency referenced to an arbitrary analysis frequency.

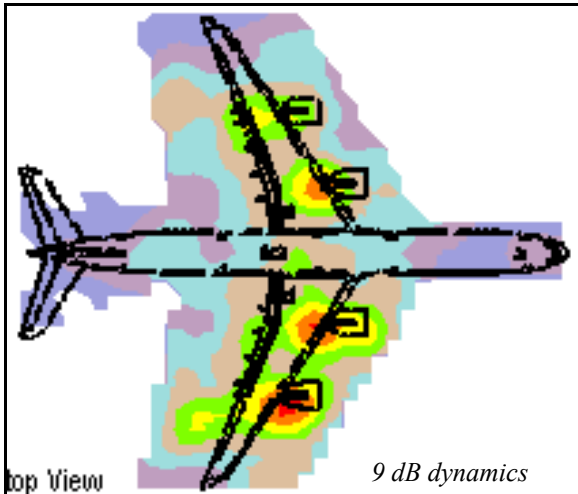


Fig. 7. Beamforming with measurements

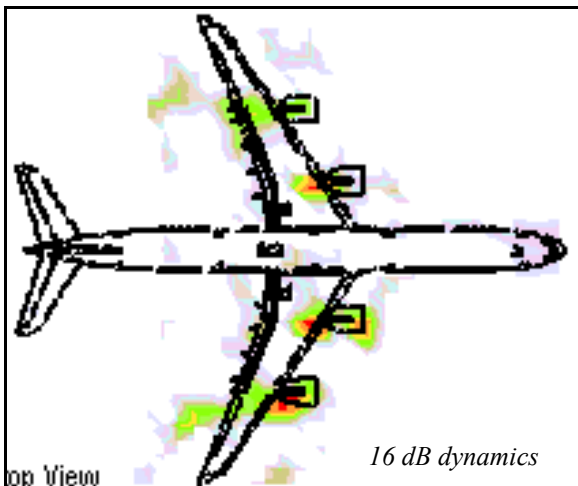


Fig. 8. Quantification with modeled sources

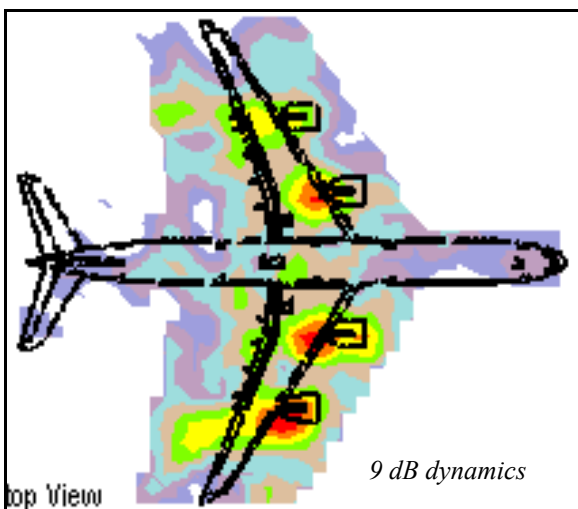


Fig. 9. Beamforming with modeled sources

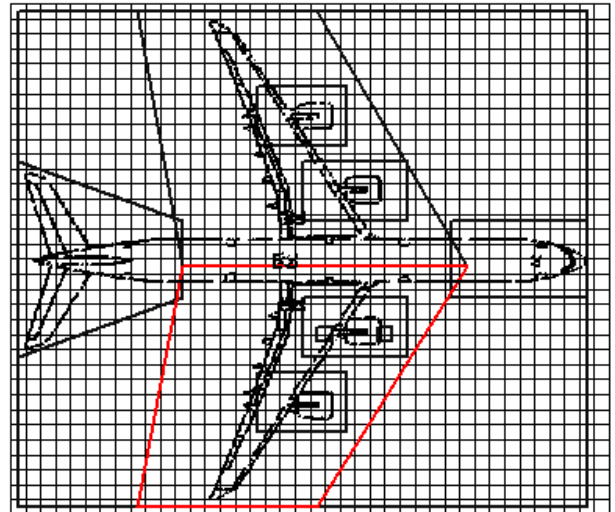


Fig. 10. Definition of zones for power spectra

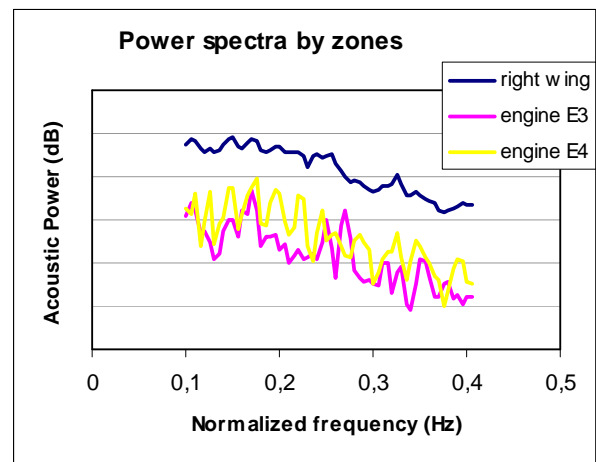


Fig. 11. Power spectra by zones

### 3.3 Doppler effect and quantification

The Doppler effect is known to affect frequency depending on the speed and the distance source-microphone. Two wave fronts emitted with a certain delay by a moving source will have this delay modified when reaching a static observer.

When starting from emission time  $t_e$ , the distance source-microphone is  $r_{s,m}(t_e)$ , and the reception time is  $t_r = t_e + r_{s,m}(t_e)/c$ . That is what is used for delayed beamforming. Received pressures  $p(t_e + r_{s,m}(t_e)/c)$  are summed in order to focus on individual point sources.

When dealing with quantification, we have to consider now a distribution of sources. The resulting pressure at each microphone at a

reception time  $t_r$  is a combination of signals emitted at different emission times  $t_e$ . We have now to find  $t_e$ , solution of  $t_r = t_e + r_{s,m}(t_e)/c$ . This implicit equation depends on the trajectory data.

On **Fig. 12**, we give a simplified linear trajectory, on which calculation of **Fig. 13** has been made. This last figure shows the link between emission time and reception time :

- ✓ in blue, the distance source microphone  $r_{s,m}$  expressed versus emission time  $t_e$  (beamforming point of view)
- ✓ in red, the distance source microphone  $r_{s,m}$  expressed versus reception time  $t_r$  (quantification point of view)

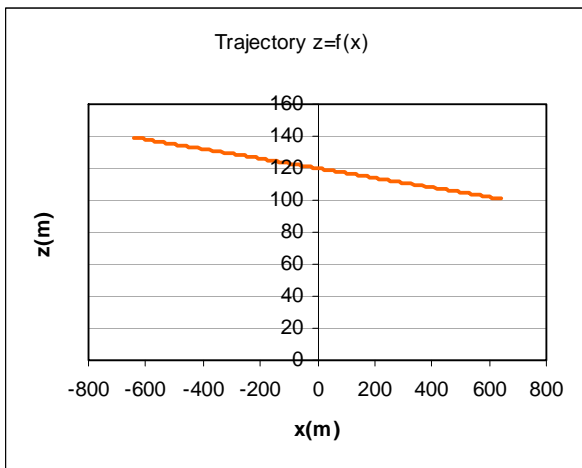


Fig. 12. Simplified trajectory

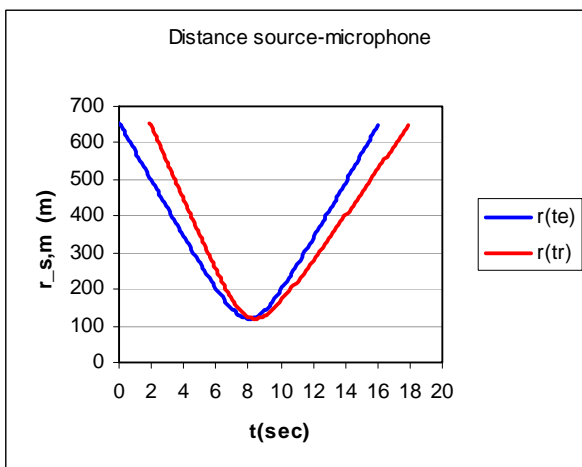


Fig. 13. Distance source-microphone expressed from beamforming point of view  $r(t_e)$ , and from quantification point of view  $r(t_r)$

## 4 Localization tests

### 4.1 Large acoustic array

The use of microphone lines needs a minimal microphone number for a good resolution and facilitates the antenna deployment. Side lobe levels are improved with processing and specific treatments between arms are performed. Different combinations of microphones lines are possible with the modular structure developed by Airbus (**Fig. 14**).



Fig. 14. View of five arm configuration

To cover the largest frequency range, the array is decomposed in several octaves dedicated embedded sub-antennas. On **Fig. 15**, the acoustic power response of several sub-antennas SA-01 to SA-04 is represented with 5dB scale. Each sub-antenna has its validity domain. Common frequency bands of consecutive sub-antennas give same power results. Global array diameter is about 50 m.

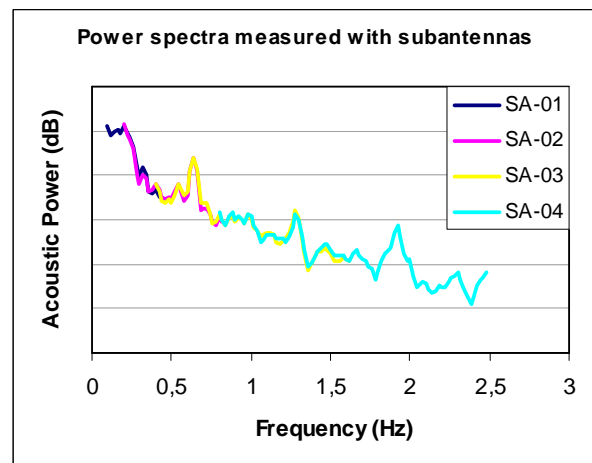


Fig. 15. Power spectra measured with sub-antennas

## 4.2 Trajectory

The aircraft real time trajectory is radio-transmitted from the aircraft and injected into acoustic software for first calculations. DGPS corrected and processed trajectory is available after end of test and used improve acoustic calculations accuracy.

## 4.3 Acquisition system

The high digitization rate of recent multi channels hardware system and high performances of processor allow a high quality dedopplerization, which is fundamental in the localization processing technique.

## 5 Conclusions

In this paper, we present a tool that has been developed by Airbus for aircraft exterior noise sources localization. The large-scale antenna can cover a wide frequency band. Low frequency sources are also described with good dynamics and resolution. The mobile and modular structure enables measurements on any test site and adapts to studied aircraft. Processing uses a three-step technique, implying a quantification of amplitude sources, which are assumed to be uncorrelated between each other. This tool now enters into a fully operational phase.

## Acknowledgements

The authors express thanks to EADS CRC, whose quantification algorithm was implemented in the processing software, and also to Company MicrodB, which was partner in the development of the processing technique.

## References

- [1] Brühl S, Röder A. Acoustic noise source modeling based on microphone array measurements. *J. Sound and Vibr.* 231(3), 611-617, 2000.
- [2] Piet J-F, Elias G. Airframe noise source localization using a microphone array. *3<sup>rd</sup> AIAA/CEAS Aeroacoustics Conference, Atlanta, GA, (USA), 12-14 May 1997, AIAA-1997-1643.*

- [3] Zillmann J, Cariou B. Array analysis for aircraft flyover measurements. *BeBeC-2010-14*, Feb 2010.
- [4] Siller H., Drescher M, Saueressig G & Lange R, Flyover source localisation on a Boeing 747-400. *BeBeC-2010-14*, Feb 2010.

## Contact Author Email Address

Authors can be contacted at following address:  
[charles.cariou@airbus.com](mailto:charles.cariou@airbus.com)

## Copyright Statement

The authors confirm that they, and/or their company or organization, hold copyright on all of the original material included in this paper. The authors also confirm that they have obtained permission, from the copyright holder of any third party material included in this paper, to publish it as part of their paper. The authors confirm that they give permission, or have obtained permission from the copyright holder of this paper, for the publication and distribution of this paper as part of the ICAS2010 proceedings or as individual off-prints from the proceedings.